06

Obtaining protective coatings based on few-layer graphene particles by chemical crosslinking

© A.A. Vozniakovskii,[1] A.P. Vozniakovskii,[2] S.I. Titova,[1] O.I. Posylkina,[3] S.V. Kidalov,[1] A.Yu. Neverovskaya,[2] E.V. Ovchinnikov[4]

[1]Ioffe Institute,
194021 St. Petersburg, Russia
[2]Lebedev Institute of Synthetic Rubber,
198035 St. Petersburg, Russia
[3]Physical Technical Institute, National Academy of Sciences of Belarus,
220141 Minsk, Belarus
[4]Yanka Kupala Grodno State University,
230023 Grodno, Belarus
e-mail: alexey_inform@mail.ru

Received October 7, 2024
Revised October 7, 2024
Accepted October 7, 2024

A new method for producing coatings based on few-layer graphene obtained under conditions of self-propagating high-temperature synthesis is described. The coating is obtained by chemical cross-linking of few-layer graphene particles by their functional groups. It has been established that these coatings can effectively protect a metal substrate from the adverse effects of strong acids.

Keywords: coatings, few-layer graphene, self-propagating high-temperature synthesis, chemical cross-linking method.

DOI: 10.61011/TP.2025.02.60827.314-24

Introduction

Fabrication of coatings is one of the most widely used material surface modification techniques that provide a material with the desired properties. However, materials that are currently used for the fabrication of coatings (metals, polymers, ceramics) aren't able any longer to satisfy current industrial needs to the full extent [1]. Therefore, researchers are looking for new materials and approaches to the synthesis of more effective coatings. More recently, many research groups have turned their attention to graphene nanostructures (GNS) [2]. The reason for this are record-breaking properties of GNS: graphene thermal conductivity is 5000 W/(m·K) [3], and Young's modulus is 1 TPa [4], while the specific surface area is estimated at 2630 m^2/g [5]. By the same reasons, researchers developed miscellaneous coatings on the basis of carbon nanotubes [6]. GNS were used to make effective protective [7], anticorrosive [8] and heat conducting [9] coatings. Two main approaches are used to make GNS-based coatings: by synthesizing GNS on a substrate and by applying pre-synthesized GNS to a substrate. In the first case, GNS are formed on a substrate using physical and chemical techniques, for example, chemical vapor deposition (CVD) [10,11] or thermal annealing of silicon carbide [12,13]. This approach is used to make high quality coatings. Low performance and expensive equipment are a substantial disadvantage of the described methods. In the second case, coating is formed from pre-synthesized GNS particles using electrophoretic deposition, spin coating [14], dip coating, etc. [15] This coating formation approach is much more effective and technically simple, while the quality of the resulting coating is highly dependent on the quality of GNS particles.

The previous study developed a new synthesis technique for few-layer graphene (FLG, maximum 5 layers) in the form of cyclic-structure biopolymer powder in the self-propagating high-temperature synthesis conditions (SHS) [16], that is free from the Stone-Wales defects [17]. Our previous studies found that FLG synthesized using this technique could effectively improve the properties of polymer composites made by DLP 3D printing [18]. Using the findings, it was supposed that the FLG made in the SHS process conditions could be used to form an effective protective coating intended for protection of metal surfaces in highly corrosive environment.

The purpose of this study was to make protective coatings from FLG particles synthesized in the SHS process conditions.

1. Materials and methods

1.1. Feedstock for coatings

FLG was used as feedstock for coatings [19]. FLG was synthesized from microcrystalline cellulose (AR, Russia). The essence of the technique is in formation of graphene planes from carbon backbones originating from various

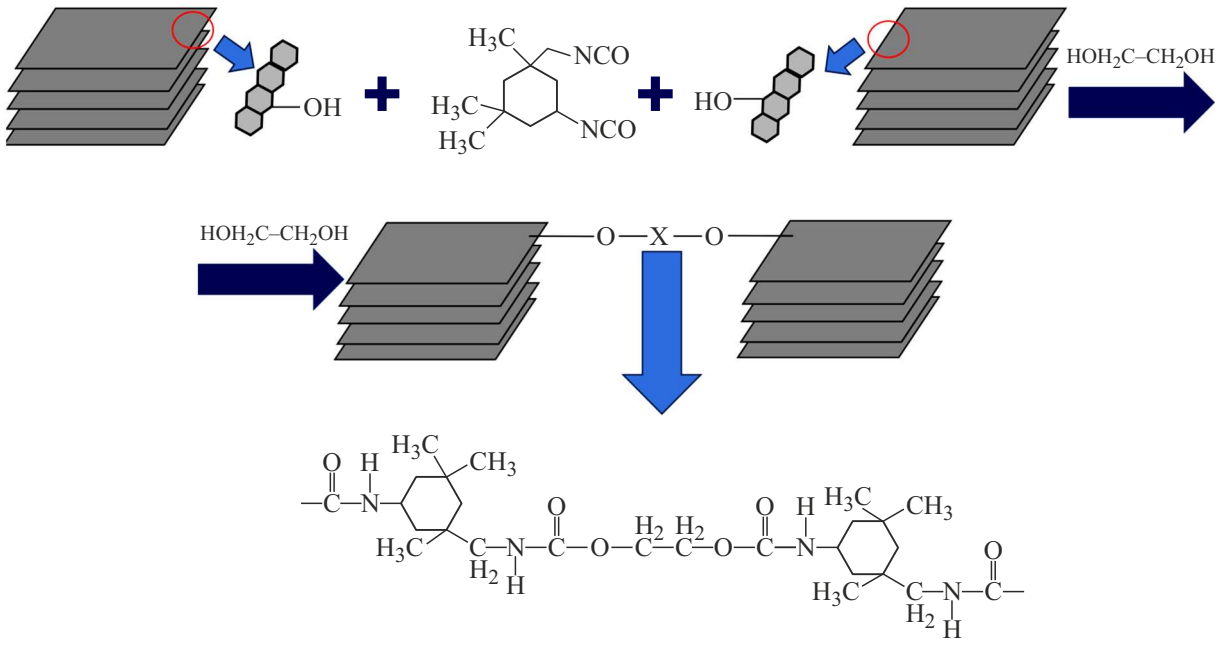


Figure 1. Flow chart of coating synthesis from FLG particles by the chemical cross-linking technique.

biopolymer molecules exposed to a high-temperature SHS wave [20]. The FLG synthesis technique is described in detail in [16].

1.2. Procedure for FLG particle coating synthesis by the chemical cross-linking technique.

The features of FLG fabrication process in the SHS conditions lead to the fact that terminal carbon atoms are closed mainly by oxygen-containing groups (−OH and −COOH). This feature was used to form cross-linked FLG particles through a diisocyanate reaction. Phenols interact with isocyanates through a concerted electrophilic addition mechanism. At the same time, hydrogen-bonding-based phenol-alcohol complexes react with isocyanates through a concerted nucleophilic addition mechanism. Phenols catalyze addition of alcohols to isocyanates. Interaction between the hydrogen-bonding-based phenol-alcohol complexes and isocyanates is kinetically and thermodynamically more preferable than reactions between isocyanates and alcohol associates [21]. From these considerations, a ternary system: FLG particles/diisocyanate/diol, was developed and put into practice to form cross-linked FLG particles (graphene coatings). Reaction scheme is shown in Figure 1.

For carboxyl groups, the reaction forms an amide bond, rather than an urethane bond [22], which also facilitates FLG particle cross-linking.

To form a durable graphene coating, an effective intermolecular bond network (chemical network) shall be made. Consequently, it was important to determine a total number of groups with an active proton in the FLG particle assembly.

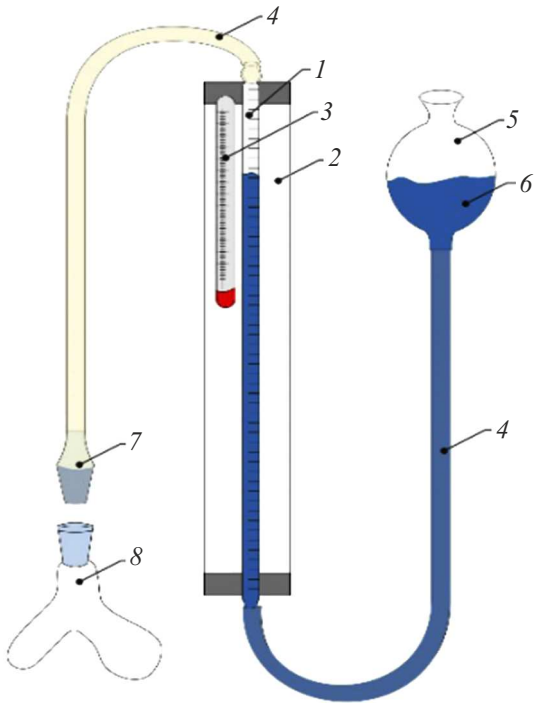


Figure 2. Upgraded system for determining the content of groups with mobile proton by the Tchugaev-Tserevitinov method. *1* — gas burette, *2* — glass jacket, *3* — thermometer, *4* — sealing liquid flexible connecting tube, funnel, *5* — flask, *6* — sealing liquid, *7* — adapter, *8* — reaction vessel.

For this, the Tchugaev-Tserevitinov reaction was used [23]. The scheme of the system upgraded for using powder-like materials is shown in Figure 2.

FLG suspension in diisoamyl ether was prepared for the reaction. The prepared suspension was mixed with the pre-synthesized Grignard reagent. The following reaction takes place during mixing:

$$\text{R-OH} + \text{CH}_3\text{MgX} \rightarrow \text{R-OMgX} + \text{CH}_4,$$

where R — is the aliphatic or aromatic radical, X — is halogen (I).

Reaction proceeds quantitatively. Calculation of groups with labile proton is based on determining the released methane volume (cm^3) during the experiment. For the FLG sample this quantity was $18.5 \pm 0.2 \cdot 10^{-3}$ mol/g.

1.3. Characterization of FLG and FLG-based coatings

Electronic images of FLG and FLG-based coatings were obtained by scanning electron microscopy using the Tescan Mira 3-M microscope (Czech Republic) with EDX detector (Oxford instruments X-max, England). The accelerating voltage was 20 eV.

FLG dispersion was measured by laser diffraction using the Mastersizer 2000 analyzer (Malverin, USA). A plate particle model was used for the measurement. For particle dispersion measurement, a suspension with a concentration of 0.05 wt.% was prepared using ultrasonic bath treatment during 5 min.

Specific surface area and porosity of FLG were measured by low-temperature nitrogen sorption using the Brunauer-Emmett-Teller method (BET) and statistical thickness method (STSA) on the Sorbi-MS meter (Russia).

Raman scattering spectra (RS) of FLG and of FLG-based coatings were recorded on the Confotec NR 500 microscope (Belarus), laser length 532 nm.

Acid resistance of coatings was studied using the following procedure: initial steel substrates and coated substrates were brought into contact with concentrated sulfuric acid (95%, 3 ml) and held in a Petri dish for 72 h (25°C, moisture 40%).

2. Findings and discussion

Figure 3 shows an electronic image of synthesized FLG particles.

Figure 3 shows that FLG powder particles form aggregates with dimensions up to several tens of microns. Some fraction of FLG particles with much smaller dimensions may be also distinguished. Laser diffraction measurements were performed to determine the particle dimensions (Figure 4).

The measurements show that the test sample contains FLG particles with sizes up to several tens of microns (particle volume distribution, Figure 4, *a*). On the other hand, the fraction of such particles is quite small and most of the FLG particles have dimensions of $0.7-1\,\mu$m, (Figure 4, *b*).

Table 1 shows the energy-dispersive analysis data.

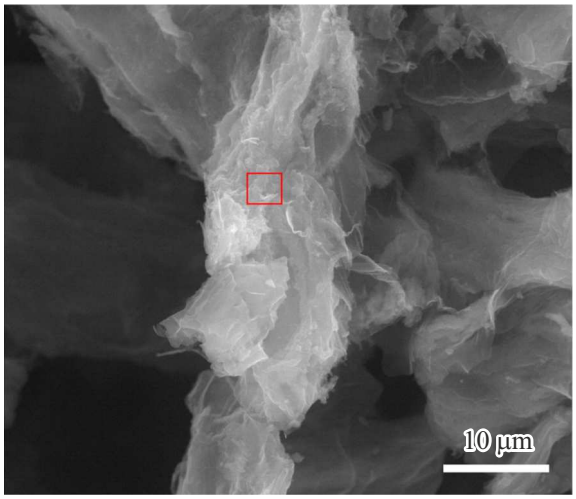


Figure 3. Electronic image of FLG synthesized from cellulose. The red square marks the area from which the signal was read during the energy-dispersive analysis.

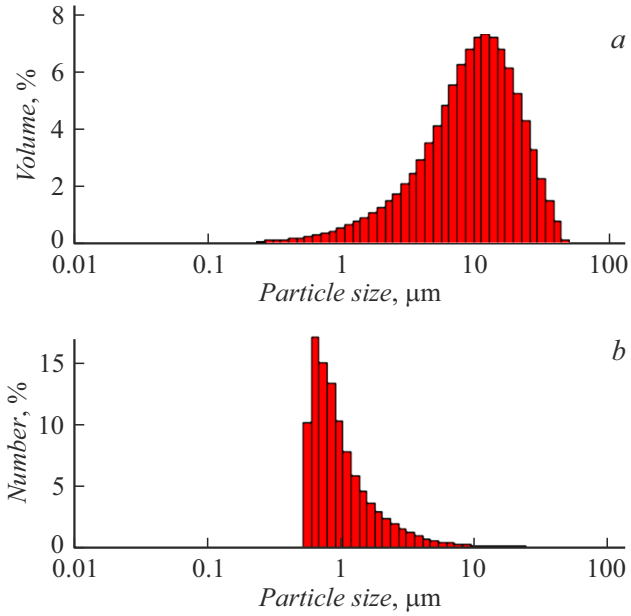


Figure 4. Distribution of FLG particles by volume (*a*) and by number of particles (*b*).

The elemental analysis data proves that the FLG sample has a composition typical for GNS: an overwhelming fraction of carbon and a small fraction of oxygen associated with the end oxygen-containing groups at the sheet edges.

Table 2 shows the specific surface area and porosity measurements of the FLG powder that was later used to form coatings.

The specific surface area of FLG measured by the STSA method is relatively small ($81\ m^2/g$), however, by accounting for the partial contribution of micropores through the BET method it was found that the total specific surface area of the sample was much larger and equal to $304\ m^2/g$.

Table 1. Elemental analysis of the FLG sample made from cellulose

Element	wt.%	at.%
Carbon	95.3 ± 0.2	95.4 ± 0.2
Oxygen	4.7 ± 0.2	4.6 ± 0.2

Figure shows an electronic cross-section image of the synthesized coating on steel substrate.

It can be seen on the electronic image that the synthesized coating is solid and has a thickness of about $70\,\mu$m.

Figure 6 shows RS spectra of the initial RS and synthesized coating.

RS spectra of initial FLG particles and FLG that form the coating are very similar and typical of GNS prepared in powder form [24,25]. *D*-peak, *G*-peak and a region containing 2*D*- and $D + G$-peaks are clearly seen on the spectra. *G*-peak in GNS is associated with extension carbon atom bonds in sp^2-hybridization, while *G*-peak is associated with the presence of various structural defects [26]. Using the intensity ratio of *D*- and *G*-peaks that is 0.81 for initial FLG, the presence of various types of defects in initial FLG particles is suggested, except the Stone-Wales defects. After formation of the coating, the intensity ratio of *D*- and *G*-peaks becomes equal to 0.86, which may indicate a minor reduction of defect content.

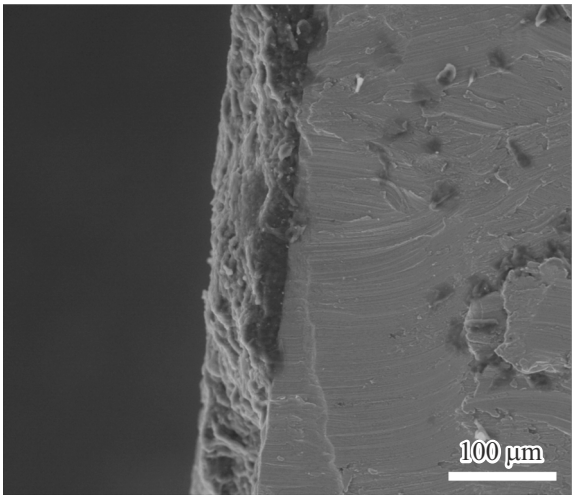


Figure 5. Electronic image of the cross-linked FLG particle coating on a steel substrate.

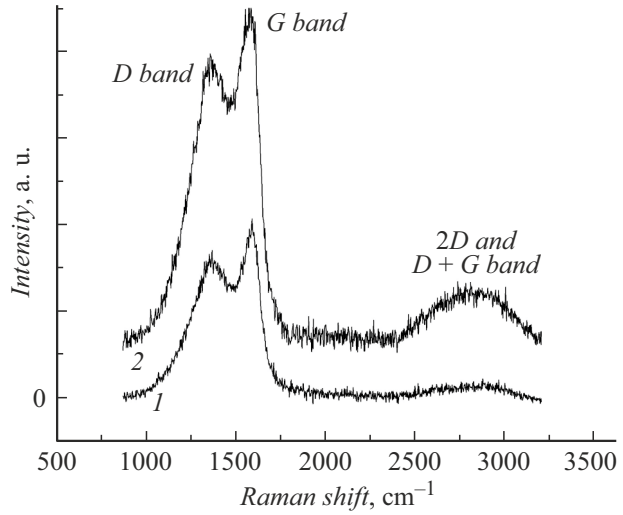


Figure 6. RS spectra of initial FLG particles (*1*) and coating (*2*).

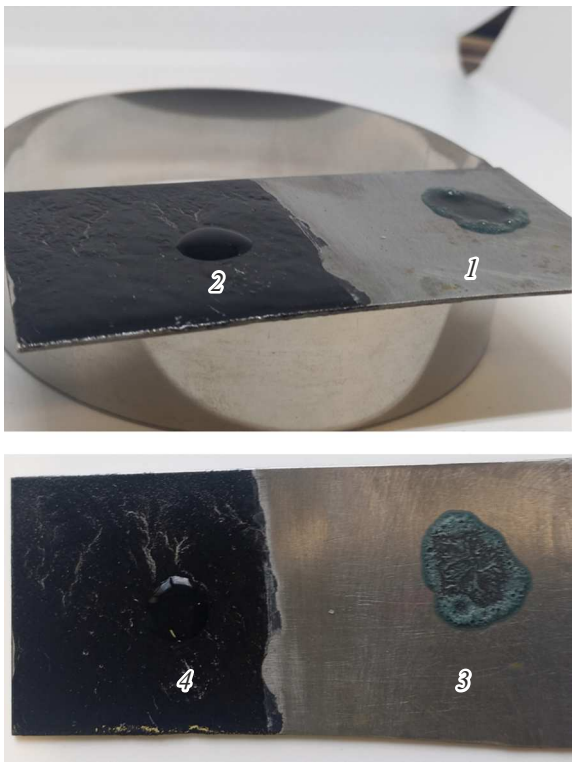


Figure 7. Acid resistance test results for cross-linked FLG particle coatings: *a* — 24 h exposure, *b* — 72 h exposure. Here, *1,3* — the steel substrate, *2,4* — the coating.

Acid test of the synthesized coatings was the key experiment of this study (Figure 7).

As shown in Figure 7, *a*, a chemical effect of sulfuric acid (corrosion) on the uncoated steel substrate is clearly seen after 24 h (1) , and is not observed in the coated region (2). After 72 h (Figure 7, *b*), corrosion in the uncoated steel substrate region is aggravated due to full consumption of sulfuric acid, while the coated region remains completely unchanged and the volume of sulfuric acid is not changed.

Conclusion

A technique of coating fabrication from FLG powder was first developed. The employed FLG feature their synthesis in the SHS process conditions.

Table 2. FLG specific surface area and porosity measurements

Specific surface area, STSA method, m^2/g	Specific surface area, BET method, m^2/g	Pore volume, cm^3/g	Micropore volume, cm^3/g
81 ± 4	304 ± 8	0.198	0.104

The FLG cross-linking method developed in the course of work can be used to easily form coating on large samples. The formed coatings represent solid coatings that effectively protect a steel substrate against adverse impact of strong acids, which suggests their high performance as protective coatings.

Future studies will investigate tribotechnical, thermophysical and electrophysical properties of coatings prepared using the chemical cross-linking technique.

Funding

The study was supported by grants of the Belarusian Republican Foundation for Fundamental Research No. T23RNFM and RNF 24-49-10014.

Conflict of interest

The authors declare no conflict of interest.

References

[1] M. Sathish, N. Radhika, B. Saleh. J. Bio Tribo-Corr., **9** (2), 35 (2023). DOI: 10.1007/s40735-023-00754-9
[2] K. Ollik, M. Lieder. Coatings., **10** (9), 883 (2020). DOI: 10.3390/coatings10090883
[3] A.A. Balandin, S. Ghosh, W. Bao, I. Calizo, D. Teweldebrhan, F. Miao, C.N. Lau. Nano Lett., **8** (3), 902 (2008). DOI: 10.1021/nl0731872
[4] C. Lee, X. Wei, J.W. Kysar, J. Hone. Sci., **321** (5887), 385 (2008). DOI: 10.1126/science.1157996
[5] Y. Zhu, S. Murali, W. Cai, X. Li, J.W. Suk, J.R. Potts, R.S. Ruoff. Adv. Mater., **22** (35), 3906 (2010). DOI: 10.1002/adma.2010010688
[6] S. Pourhashem, E. Ghasemy, A. Rashidi, M.R. Vaezi. J. Coat. Technol. Res., **17** (1), 19 (2020). DOI: 10.1007/s11998-019-00275-6
[7] B. Kulyk, M.A. Freitas, N.F. Santos, F. Mohseni, A.F. Carvalho, K. Yasakau, A.J.S. Fernandes, A. Bernardes, B. Figueiredo, R. Silva, J.T.F.M. Costa, Crit. Rev. Solid State Mater. Sci., **47** (3), 309, (2022). DOI: 10.1080/10408436.2021.1886046
[8] R. Zhang, X. Yu, Q. Yang, G. Cui, Z. Li. Constr. Build. Mater., **294**, 123613 (2021). DOI: 10.1016/j.conbuildmat.2021.123613
[9] P. Huang, Y. Li, G. Yang, Z.-X. Li, Y.-Q. Li, N. Hu, S.-Y. Fu, K.S. Novoselov. Nano Mater. Sci., **3** (1), 1 (2021). DOI: 10.1016/j.nanoms.2020.09.001
[10] N.A. Nebogatikova, I.V. Antnova, R.A. Soots, K.A. Kokh, E.S. Klimova, V.A. Volodin. ZhTF, **92** (4), 261 (2024). (in Russian) DOI: 10.61011/JTF.2024.02.57081.281-23
[11] A.B. Loginov, R.R. Ismagilov, A.N. Obraztsov, I.V. Bozhev, S.N. Bokova-Sirosh, E.D. Obraztsova, B.A. Loginov. Tech. Phys., **64** (11), 1666 (2019). DOI: 10.1134/S1063784219110185
[12] S.P. Lebedev, S.Iu. Priobrazhenskii, A.V. Plotnikov, M.G. Mynbaeva, A.A. Lebedev. Tech. Phys., **68** (12), 648 (2022). DOI: 10.1134/S1063784223080169
[13] S.P. Lebedev, I.S. Barash, I.A. Eliseyev, P.A. Dementev, A.A. Lebedev, P.V. Bulat. Tech. Phys., **64** (12), 1843 (2019). DOI: 10.1134/S1063784219120144
[14] O. Kwon, Y. Choi, E. Choi, M. Kim, Y.C. Woo, D.W. Kim. Nanomaterials, **11** (3), 757 (2021). DOI: 10.3390/nano11030757
[15] X. Gu, Y. Zhao, K. Sun, C.L. Vieira, Z. Jia, C. Cui, Z. Wang, A. Walsh, S. Huang. Ultrason. Sonochem., **58**, 104630 (2019). DOI: 10.1016/j.ultsonch.2019.104630
[16] A.P. Voznyakovskii, A.A. Vozniakovskii, S.V. Kidalov. Nanomaterials, **12** (4), 657 (2022). DOI: 10.3390/nano12040657
[17] A.P. Voznyakovskii, A.A. Neverovskaya, A.A. Vozniakovskii, S.V. Kidalov. Nanomaterials, **12** (5), 883 (2022). DOI: 10.3390/nano12050883
[18] S. Kidalov, A.P. Voznyakovskii, A.A. Vozniakovskii, S. Titova, Y. Auchynnikau. Materials, **16** (3), 1157 (2023). DOI: 10.3390/ma16031157
[19] *Nanotechnologies — Structural characterization of graphene — Part 1: Graphene from powders and dispersions* ISO/TS 21356-1
[20] A.P. Voznyakovskii, A.A. Vozniakovskii, S.V. Kidalov. Fullerenes, Nanotubes Carbon Nanostruct., **30** (1), 59 (2022). DOI: 10.1080/1536383X.2021.1993831
[21] S.V. Nesterov. *Vliyanie fenolnykh soedinenii na protsess obrazovaniya poliuretanov i ikh termicheskuiyu stabilnost* (Avtoref. diss., 2013)
[22] J.H. Saunders, K.C. Frish, Khimiya poliuretanov, Per. s angl. Z.A. Kochnovoi, Zh.T. Korkishko, pod.red. S.G. Entelisa (Izd-vo Khimiya, M., 1968), 470 s. (in Russian)
[23] S.T. Ioffe, A.N. Nesmeyanov. *Metody elementoorganicheskoy khimii* (Izd-vo AN, M., 1963), 562 s. (in Russian)
[24] F.T. Johra, J.W. Lee, W.G. Jung. J. Ind. Eng. Chem., **20** (5), 2883 (2014). DOI: 10.1016/j.jiec.2013.11.022
[25] S. Perumbilavil, P. Sankar, T. Priya Rose, R. Philip. Appl. Phys. Lett., **107** (5), 051104 (2015). DOI: 0.1063/1.4928124
[26] Z. Li, L. Deng, I.A. Kinloch, R.J. Young. Prog. Mater. Sci., **135**, 101089 (2023). DOI: 10.1016/j.pmatsci.2023.101089

Translated by E.Ilinskaya